

**Theoretical evaluation on burn injury of human  
respiratory tract due to inhalation of  
hot gas at the early stage of fires<sup>1</sup>**

Yong-gang Lv<sup>1,2</sup>, Jing Liu<sup>1\*</sup>, and Jun Zhang<sup>3</sup>

- 1) Cryogenic Laboratory, P. O. Box 2711, Technical Institute of Physics and Chemistry,  
Chinese Academy of Sciences, Beijing 100080, P. R. China
- 2) Graduate School of the Chinese Academy of Sciences, Beijing 100039, P. R. China
- 3) Laboratory for High Performance Scientific Computing and Computer Simulation,  
Department of Computer Science, University of Kentucky, 773 Anderson Hall,  
Lexington, Kentucky 40506-0046, USA

February 23, 2005

\*Address for correspondence:

Dr. Jing Liu  
Cryogenic Laboratory, P. O. Box 2711  
Technical Institute of Physics and Chemistry,  
Chinese Academy of Sciences,  
Beijing 100080, P. R. China  
Email address: [jliu@cl.cryo.ac.cn](mailto:jliu@cl.cryo.ac.cn)

---

<sup>1</sup> Technical Report No. 435-05, Department of Computer Science, University of Kentucky, Lexington, KY, 2005.

Tel. +86-10-62639266

Fax: +86-10-62554670

### **Abstract**

A transient two-dimensional mathematical model for the heat and water vapor transport over the respiratory tract of human body was established and applied to predict the thermal impact of inhaled hot air during the early stage of fires. Influences of individual's physiological status and environment variables were comprehensively investigated. Burn evaluation was performed using the classical Henriques model to predict the time for thermal injury. It was shown that decreasing the air velocity and increasing the respiratory rate is helpful to minimize the thermal injury in the respiratory tract. The effect of relative humidity of surrounding dry hot air could be ignored in predicting the burn injuries for short duration exposures. Due to evaporation cooling on the mucousal membrane, the burn injury often occurs at certain positions underneath the skin of the tract near the inlet of the respiratory tract. Most of the tissues near the surface suffer injury immediately after exposure, while in the deeper tissues, serious damage occurs after a relatively longer time period. The method presented in this paper may suggest a valuable approach to theoretically evaluating the injury of hot air to the human respiratory tract under various fire situations.

**Keywords:** Burn evaluation; Fire injury; Theoretical evaluation; Respiratory tract;  
Bioheat transfer

### **Nomenclature**

$A$	Airway cross section ( $\text{m}^2$ )
$C$	Specific heat of tissue ( $\text{J/kg} \cdot \text{K}$ )
$C_A$	Specific heat of air ( $\text{J/kg} \cdot \text{K}$ )
$C_b$	Specific heat of blood ( $\text{J/kg} \cdot \text{K}$ )
$H$	Latent heat of water vaporization ( $\text{J/kg}$ )
$h_f$	Heat convection coefficient between the mucousal surface and flowing air stream ( $\text{W/m}^2 \cdot \text{K}$ )
$h'_f$	Heat convection coefficient between the tissue and the surrounding air ( $\text{W/m}^2 \cdot \text{K}$ )

$K$	Thermal conductivity of tissue (W/m · K)
$L$	Longitudinal length of human respiratory tract (m)
$m$	Water penetrative coefficient in mucosal surface (kg/s · m <sup>2</sup> · Pa)
$Nu$	Nusselt number
$p$	Air perimeter (m)
$P$	Pre-exponential factor (s <sup>-1</sup> )
$P_a^*$	Saturated vapor pressure at surrounding air temperature (kPa)
$P_{sk}^*$	Saturated vapor pressure at tissue temperature (kPa)
$Q_m$	Metabolic rate of tissue (W/m <sup>3</sup> )
$R$	Ideal gas constant (J/mol · K)
$Re$	Reynolds number
$r$	Radial position (m)
$Sc$	Schmidt number
$t$	Time (s)
$T$	Temperature (K)
$T_a$	Artery temperature (°C)
$T_A$	Air temperature (°C)
$T_{A0}$	Initial air temperature (°C)
$T_0$	Steady-state temperature of tissue (°C)
$T_f$	Surrounding air temperature (°C)
$T_{f0}$	Initial surrounding air temperature (°C)
$T^*$	Duration of a complete cycle of inspiration and expiration (s)
$V$	Local mean volumetric longitudinal air velocity (m <sup>3</sup> /s)
$v$	Local mean longitudinal air velocity (m/s)
$W_b$	Tissue blood perfusion (kg/ m <sup>3</sup> · s)
$z$	Axial position (m)
$\Omega$	Dimensionless Henriques' burn integral

### Greek symbols

$\Delta E$	Activation energy (J/mol)
$\rho$	Density of tissue (kg/ m <sup>3</sup> )
$\rho_A$	Density of air (kg/ m <sup>3</sup> )
$\alpha$	Thermal diffusivity of tissue (m <sup>2</sup> /s)

$\varphi$  Relative humidity of surrounding air

## 1. Introduction

Burn injury due to inhalation of hot gas is commonly encountered in clinics, which may significantly threaten the recovery of fire victims, claiming thousands of deaths in the USA alone [1]. Children, young adults, and the elderly are the most likely victims [2]. Therefore various clinical therapies have been designed to improve survival of patients with burn injury. Strategies have also been proposed to evaluate the potential injuries of people subject to instantaneous and strong fire and thus to lower the dangers of fire injury. Over the past few decades, tremendous advances in burn care have contributed to a decrease in burn mortality. The new approaches include, but are not limited to, fluid resuscitation formulas [3], nutritional support regimes [4,5], high frequency oscillatory ventilation [6], introduction of localized antimicrobials, early surgical excision of eschar to reduce the occurrence of sepsis [7], and new management regimes of life-threatening hypermetabolic response to large burns [8,9]. However, to the best of our knowledge, no specific therapy for the combined burn and smoke inhalation injury has yet been established.

As one of the most serious reasons to cause human death, the mechanisms for the inhalation injury can be attributed to a combination of thermal, hypoxaemic and chemical effects of the hot smoke [10]. Thermal injury to the respiratory tract is usually limited to upper the vocal cords. Low heat capacity of the dry air and reflex adduction of the vocal cords would protect the lower airways from thermal injury [10,11]. Clearly, a better understanding of the interplay between transient temperature and injury distributions over the human respiratory tract may help to yield a well-directed treatment in the near future. Under normal breathing conditions, the nose and/or mouth would heat and moisten the inhaled air so that its temperature appears often close to the body temperature. This area usually saturates with water vapor, and recovers some of the heat and water vapor transported by the air during the expiration phase. This conditioning of the inspired air is accomplished as the air-stream flow through the respiratory tract exchanging heat and water with the mucus membrane lining the airway surfaces. The process is remarkably stable over a range of inspiratory air temperature between  $-100^{\circ}\text{C}$  and  $500^{\circ}\text{C}$  [12,13]. The air-conditioning process does not occur uniformly throughout the respiratory system. Most of the respiratory

air-conditioning occurs in the upper respiratory tract, as shown in a previous study [14-17]. The process of thermal injury takes place quickly and the resulted injury often occurs at the early stage of fires. Accurate predictions of the early temperature elevation are, thus, very critical to evaluate the burn injury in human respiratory tract under a fire. It also helps understand what people should do to minimize lung damage when exposed to fires. Therefore, the transient air temperature history across the nose and mouth plays an important role in the thermal injury during fires. Although there have been many literature to perform numerical simulation on the skin burn injury, few efforts were ever made to analyze the burn process of the human upper respiratory tract up to now. In this study, a transient theoretical model is established to describe the local heat transport and quantify the burn degree along the airway during the fires. The results would help better understand the development of heat injury taking place in the respiratory tract exposed to various fire situations. To minimize the lung injury when exposed to a fire or natural disaster, the time for the first-degree burns to occur is also theoretically predicted. Further, the effect of blood perfusion rate, thermal conductivity, volumetric metabolic heat of tissue, velocity and relative humidity of surrounding air and respiratory frequency is also tested.

## **2. Theoretical model**

Analysis of heat and water transport process in the respiratory tract is generally a tough task because the flow patterns inside this area is rather complex. For simplicity, the airway can be idealized as a long, right circular cylinder (Fig. 1). Such simplified structure had also ever been used before by some other authors [14]. This is a simple however very useful treatment, which would make the theoretical analysis feasible. The tissue temperature is considered as continuous functions of axial ( $z$ ) and radial ( $r$ ) positions and time ( $t$ ), while the air temperature is only the continuous functions axial ( $z$ ) position and time ( $t$ ). Based on the well known Pennes bioheat transfer equation, the transient theoretical model for the present problem can be derived by applying conservation of energy to a “slice” across the airway, as shown schematically for inspiration in Figure 1.

For the tissue area, the resulting equation is set up as follows:

$$\frac{1}{\alpha} \frac{\partial T}{\partial t} = \frac{\partial^2 T}{\partial r^2} + \frac{1}{r} \frac{\partial T}{\partial r} + \frac{\partial^2 T}{\partial z^2} + \frac{W_b C_b}{K} (T_a - T) + \frac{Q_m}{K} \quad (1)$$

where,  $\alpha = K/\rho C$  is the diffusivity of tissue,  $\rho, C, K$  are respectively the density, specific heat and thermal conductivity of the tissue;  $C_b$  denote specific heat of blood;  $W_b$  the blood perfusion;  $T_a$  the supplying arterial blood temperature which is treated as a constant, and  $T$  the tissue temperature, and  $Q_m$  the metabolic heat generation rate.

During a real thermal process, the boundary condition (BC) at the tract skin surface is often time-dependent. At this mucous-air interface ( $r = a$ ), the generalized boundary condition for the heat transfer is generally composed of two parts, i.e., convection and evaporation. At the entrance of the nasal cavity ( $z = 0$ ), the continuity of the perpendicular heat flux has been imposed as a convective boundary condition. The thermoregulation mechanisms of the biological bodies have been neglected because of the slight temperature increase induced. For solving the problem, heat flux is assumed to approach zero at both the deep tissue ( $r = b$ ) and the end of the human respiratory tract ( $z = L$ ), which is also realistic for biological body. Then the boundary conditions (BC) can be written as follows:

$$K \frac{\partial T}{\partial r} = h_f (T - T_A) + Hm(p_{sk}^* - \varphi p_a^*), \quad r = a \quad (1a)$$

$$\frac{\partial T}{\partial r} = 0, \quad r = b \quad (1b)$$

$$K \frac{\partial T}{\partial z} = h'_f (T - T_f), \quad z = 0 \quad (1c)$$

$$\frac{\partial T}{\partial z} = 0, \quad z = b \quad (1d)$$

and the initial condition (IC) is

$$T = T_0, \quad t = 0 \quad (1e)$$

where,  $T_0$  is steady-state temperature field, which is assumed as the uniform value  $T_a$ ;  $T_f$  is the surrounding hot air temperature;  $h'_f$  is the apparent heat convection coefficient between the tissue and the surrounding air and  $h_f$  the heat convection coefficient between the mucousal surface and the flowing air stream;  $\varphi$  is the relative humidity of surrounding air;  $H$  is the

latent heat of water vapour;  $m$  is water penetrative coefficient in mucosal surface;  $P_a^*$  is the saturated vapor pressure at surrounding air temperature and  $P_{sk}^*$  the saturated vapor pressure at tissue temperature. In the above equations, the unit for pressure is kPa.

In the respiratory tract, the air temperature gradients in the axial direction are usually much smaller than that in radial direction. Correspondingly, the axial conduction is neglected here for simplicity. Inclusion of axial conduction to conduct a more strict analysis needs further research in the near future. Then the energy balance equation for the air can be obtained as

$$\frac{\partial T_A}{\partial t} = -v(t, z) \frac{\partial T_A}{\partial z} + \frac{p(z)}{\rho_A C_A A(z)} [h_f (T - T_A) + rm (p_{sk}^* - \phi p_a^*)] \quad (2)$$

where,  $C_A$  and  $\rho_A$  are respectively the specific heat and density of the air;  $A(z)$  and  $p(z)$  are the local airway cross section and perimeter, respectively;  $v(t, z)$  the local mean longitudinal air velocity ( $v(t, z) = V/A$ ), and  $V$  the local volumetric longitudinal air velocity.

During the inspiration phase, the axial inlet boundary conditions at  $z = 0$  can be considered as the boundary air temperature ( $T_f$ )

$$T_A = T_f, \quad z = 0 \quad (3a)$$

During and expiratory phase of the breathing cycle, the heat flux is assumed to approach zero at the end of the human respiratory tract ( $z = L$ ). The boundary condition for expiration is therefore listed as follows

$$\frac{\partial T_A}{\partial z} = 0, \quad z = L \quad (3a')$$

The burn process is modeled using the following initial condition:

$$T_A = T_{A0}, \quad t = 0 \quad (3b)$$

To calculate the transient air temperature field, the initial air temperature distribution  $T_{A0}$  before inhalation injury needs to be known. It can be obtained by solving Eq. (2) with the following boundary conditions:

$$T_{A0} = T_{f0}, \quad z = 0 \quad (3c)$$

in which  $T_{f0}$  is the initial surrounding air temperature.

### 3. Results and discussion

#### 3.1. Solution strategy and model parameters

A predictor-corrector numerical method is applied to solve the above equations. The space and time steps are small enough to ensure that the transient temperatures are mesh-independent. Blood perfusion, thermal conductivity, and heat capacity are assumed to be constant in the tissue despite the temperature elevation. In the following calculation, the typical values for tissue and air properties are taken as [18]

$$\begin{aligned} \rho &= 1000 \text{ kg/m}^3, \quad C = C_b = 4000 \text{ J/kg} \cdot \text{K}, \quad T_a = 37^\circ \text{C}, \quad K = 0.5 \text{ W/m} \cdot \text{K}, \\ W_b &= 0.5 \text{ kg/m}^3 \cdot \text{s}, \quad Q_m = 420 \text{ W/m}^3, \quad h'_f = 50 \text{ W/m}^2 \cdot \text{K}, \quad L = 6 \text{ cm}, \quad T_{f0} = 20^\circ \text{C}, \\ T_f &= 100^\circ \text{C}, \quad a = 0.635 \text{ cm}, \quad b = 3.635 \text{ cm}, \quad V = 300 \text{ cm}^3/\text{s}, \quad \phi = 0.3, \quad H = 2430.9 \times 10^3 \text{ J/kg} \\ m &= 1.271 \times 10^{-6} \text{ kg/s} \cdot \text{m}^2 \cdot \text{pa}, \quad C_A = 1005 \text{ J/kg} \cdot \text{K}, \quad \rho_A = 1.165 \text{ kg/m}^3, \end{aligned}$$

The heat convection coefficient  $h_f$  between the mucousal surface and the flowing air stream is evaluated from physiological data by naphthalene sublimation experiment [14]. The values for inspiration and expiration can be obtained from the following equations respectively.

For inspiration phase:

$$Nu = 0.056 \text{ Re}^{0.856} Sc^{1/3} \quad (4a)$$

For expiration phase:

$$Nu = 0.017 \text{ Re}^{0.984} Sc^{1/3} \quad (4b)$$

When the temperature falls in between  $0^\circ\text{C}$  and  $200^\circ\text{C}$ , an accurate approximation to saturated vapor pressure is [19]:

$$\ln(1000 \times P^*) = \frac{C_1}{T} + C_2 + C_3 T + C_4 T^2 + C_5 T^3 + C_6 \ln(T) \quad (5)$$

where,

$$\begin{aligned} C_1 &= -5800.2206, \quad C_2 = 1.3914993, \quad C_3 = -0.04860239, \\ C_4 &= 0.41764768, \quad C_5 = -0.1442093 \times 10^{-7}, \quad C_6 = 6.5459673. \end{aligned}$$

In the normal respiration, the air is taken in through the nostrils without making any special effort, and sound or exaggerated movement of the nose or chest. In short, it is done unconsciously. Breathing is a cyclic phenomenon. The air temperature oscillates with alternative inspiration and expiration. The duration of a complete cycle of inspiration and expiration normally takes about 3 seconds, and the frequency of respiration is about 20 breaths/minute, in a resting normal adult, at sea level.

### 3.2. Temperature responses of tissues and air in human nasal tract during a fire

Depicted in Fig. 2 is the steady state temperature distribution of tissues along the airway in normal conditions. It can be seen that, the air temperature increases with the distance away from the nose and at about the main bronchial generation ( $z = 18 \text{ cm}$ ), it reaches about 90 percent of the body temperature during the inspiration phase. The heat loss associated with the latent heat of the water vaporization may results in a local drop in temperature. For convenience, the mucosal

temperature is assumed to be a constant in normal condition. However, it will be seriously varied by the inhaled surrounding hot air when a person is exposed to a fire or natural disaster. Figs. 3 and 4 give the transient temperature distribution in tissue and air after the exposure. Clearly, the surface tissue temperature increases immediately after the exposure, while in the deeper tissues, the temperature increases slightly until after a longer period of time. This is consistent with our normal cognition. Thermal injury occurs on exposed external surface areas including nose and mouth; burns below the trachea are nearly not encountered due to the efficiency of the upper airway in absorbing the heat. Fig. 3 still indicates that, there seems no temperature fluctuations throughout the inspiratory and expiratory phases of the breathing cycle. The reason can be attributed to the high air speed and thermal capacity of tissue. On the one hand, the air velocity during the inspiratory and expiratory phases of the breathing cycle is so high that heat exchange between air and mucosal can quickly reach its steady state. Another reason lies in that, thermal capacity of the tissue is much higher than that of the air. However, this small fluctuation can be seen clearly in Fig. 5. Due to heat loss to the tissue, the air temperature decreases absurdly from the inlet of respiratory tract to the outlet during an inspiration phase. However, the air temperature remains almost the same over the expiration stage (Fig. 4). The temperature of the inspired air is decreased to that near the body core temperature ( $37^{\circ}\text{C}$ ). Thus, almost no heat exchange occurs during expiration.

In order to show the tissue temperature fluctuation clearly, transient tissue temperature responses at two specific positions  $z = 8\text{cm}$ ,  $r = 0.635\text{cm}$  and  $z = 52\text{cm}$ ,  $r = 0.635\text{cm}$  are particularly given in Fig. 5. One can see that the higher amplitude of the temperature oscillation occurs at the position near the inlet of the respiratory tract. Fig. 6 gives out the transient air temperature responses at the two sections  $z = 8\text{cm}$  and  $z = 52\text{cm}$ . The oscillations are much larger than that of the tissue temperature due to low thermal capacity of the air. In the inlet of the respiratory tract, the air temperature is mainly influenced by the surrounding air. Thus, the highest temperature almost does not change during inspiration. However, the influence of the surrounding air will become weak near the outlet of the respiratory tract where the highest and the lowest air temperatures both gradually increase with the increase of time.

### *3.3. Influence of individual's physiological status and environment variables*

Many factors influence environmental effects on tissue temperature response. The individual's psychology and physiology are also important. Parametric analysis on these factors will help to appropriately address the burn injury issue.

Different people such as young or old have different blood perfusion rate. Even the same person has a varied blood perfusion at various health statuses. Clearly, as the main heat transfer path, the blood perfusion level will affect the biological response to a fire. Fig. 7 depicts the tissue temperature responses corresponding to three different blood perfusion levels. For the case of  $W_b = 5.0 \text{ kg} / \text{m}^3 \cdot \text{s}$ , the tissue temperature appears much smaller than that of using  $W_b = 0.05 \text{ kg} / \text{m}^3 \cdot \text{s}$

at the same position. It can be seen that large blood perfusion tends to prevent the biological body from burn injury. From this point, one can predicate that an old person, whose perfusion is generally lower, is easier to be injured by a fire than a young person is. This is because the higher blood perfusion compensates for the heat production by the external surrounding air heating. In the same time, one can find that the time for the tissue temperature to reach a steady state is shorter when the blood perfusion is higher. For the case of  $W_b = 0.5 \text{ kg} / \text{m}^3 \cdot \text{s}$ , about 300s is needed for the tissue temperature to reach a steady state. However, when the blood perfusion is lower ( $W_b = 0.05 \text{ kg} / \text{m}^3 \cdot \text{s}$ ), a much longer time is needed. The result can help explain the fact that the elderly [2] are among the most likely victims in terms of thermal injury. Further calculation shows the influence of the thermal conductivity on the tissue temperature response. The tissue temperature increases with the increase of the thermal conductivity of tissue. The temperature of the surface tissue will be closer to the body core temperature when the thermal conductivity becomes high enough. In fact, the thermal conductivity of the tissue depends on its components. The water in the tissue may affect the thermal conductivity of the respiratory tract. Usually, the thermal conductivity of tissue will decrease with the loss of water. This may imply that the thermal injury will be more serious if taking into concern the decrease of the thermal conductivity due to water loss. Fig. 9 gives the temperature responses in tissue at a specific position ( $z = 8\text{cm}$ ,  $r = 0.635\text{cm}$ ) with different metabolic rates. Clearly, the larger the metabolic rate, the higher the temperature increases. This suggests that keeping calm is helpful to minimize the thermal injury in respiratory tract.

In order to supply enough amount of oxygen for lung, the respiratory rate may tend to increase after exposure in a fire. As shown in Fig. 10, the tissue mean temperatures do not display evident difference under various respiratory rates. It is noticed that the amplitude of the temperature oscillation can increase with the decrease of the respiratory rate. With the decrease of the respiratory cycle (RC), heat received by the respiratory air from the deeper tissue of nasal mucosal is not sufficiently large because of the high-speed flowing air during the inspiratory and expiratory phases of the breathing cycle. Further calculation indicates that relative humidity of the surrounding air has no significant effect on the thermal injury in the respiratory tract for short duration exposures. The reason lies in that the heat loss at the mucosal surface due to evaporation is much less than that due to convection when the surrounding air is dry and hot.

Apart from the above factors, the environmental variables, such as the surrounding air temperature also plays a key role in deciding the thermal injury. Too hot environment will cause quick thermal injury in respiratory tract. For the case of  $T_f = 150^\circ\text{C}$ , the temperature of tissue at  $z = 8\text{cm}$ ,  $r = 0.635\text{cm}$  will become  $48^\circ\text{C}$  at 300s. However, when the surrounding air temperature is  $70^\circ\text{C}$ , the temperature of tissue at the same position is only  $39^\circ\text{C}$  (Fig. 11). As it appears, the temperature of the surrounding air has an important effect on the thermal injury in respiratory tract. A healthy man will lose consciousness quickly when the surrounding air

temperature reaches about 150°C [20].

Fig. 12 illustrates the effect of local mean longitudinal air velocity on temperature response at a specific position ( $z = 8\text{cm}$ ,  $r = 0.635\text{cm}$ ). Different from the effect of the respiratory rate, a higher air velocity can increase the tissue temperature absurdly. From this point, decreasing the air velocity and increasing respiratory rate is helpful for minimizing the thermal injury in respiratory tract.

### 3.4. Burn evaluation

It is generally accepted that thermal damage begins when the tissue temperature rises above 44°C [21]. Quantitative burn degree evaluation was first proposed by Henriques [22] based on that the tissue damage can be represented as an integral of a chemical rate process

$$\Omega = \int_0^t P \exp\left(-\frac{\Delta E}{RT}\right) \cdot dt \quad (6)$$

where,  $P$  is a constant that varies with tissue and local temperature,  $\Delta E$  and  $R$  are the activation energy and idea gas constant, as given in Table 1. If both conditions of  $T > 44^\circ\text{C}$  and  $\Omega > 0.53$  are satisfied at the entrance of the human respiratory tract ( $z = 0$ ), then it is defined as the first-degree burn. In the following, burn times are predicted based on the integral constants given by Henriques [22]. Fig. 13 is the dimensionless Henriques' burn integral distribution at the surface of tissue ( $0.635\text{cm} \leq r \leq 3.635\text{cm}$ ) during a fire. As shown in Figure 13,  $\Omega$  at the inlet of the nasal cavity increases from 0 to 40 within 800 seconds. Obviously, due to the surface water evaporation cooling, the burn injury often occurs at certain positions underneath the skin surface near the inlet of respiratory tract. Most of the tissues near the surface suffer injury immediately after the exposure, while in the deeper tissues, serious damage occurs after a relatively longer time period. Fig. 14 indicates the first-degree burn time predicted by equation (6). At the nasal mucosal surface ( $r = 0.635\text{cm}$ ), the first-degree burn will occur only after 230s, while more than 900s is needed for the first-degree burn to occur at a deeper tissue ( $r = 0.935\text{cm}$ ). All these differences are caused by the thermal development of the hot air heating. Clearly, facing the fire, the human upper respiratory tract will easily subject to serious burn if a quick enough getting away from the fire ground was not successful.

## 4. Conclusion

In order to predict the air temperature response in the nasal cavity, a transient theoretical model was described to interpret the thermal injury at the early stage of fires. Effects of the individual's physiological and environmental variables (such as blood perfusion, thermal conductivity, metabolic rate, air temperature, air velocity, and respiratory rate) were investigated

in detail. According to the numerical results, decreasing the air velocity and increasing respiratory rate is helpful to minimize the thermal injury in respiratory tract. The effect of relative humidity of surrounding air can be ignored in predicting the burn injuries for short duration exposures. Further, burn times are predicted based on the classical evaluation criterion. Most of the tissues near the surface suffer injury immediately after the exposure, while in the deeper tissues, serious damage occurs after a relatively longer time period. However, several limitations in this study should be pointed out. For example, more complex geometrical and physiological parameters of the respiratory system may be incorporated for a more comprehensive prediction. The present model, mainly developed here for characterizing the situations at early stage of fire, still could not be directly used to study the heat transfer process when the nasal tract has been completely burned. In that case, tissue parameter and the equations need to be modified. Further, the present model had not included the effects of the densely wet hot air such as the inhaled water vapor. For that purpose, phase change heat transfer must be considered to address such water evaporation. These problems will be studied in our later research. Studies performed in this paper warrant further investigation along this direction.

## **Acknowledgements**

This work is partially supported by the National Natural Science Foundation of China under grant 50325622.

## **References**

- [1] Pruitt Jr. BA, Goodwin CW, Mason Jr. AD. Epidemiological, demographic and outcome characteristics of burn injury. In: Herndon DN, editor. *Total Burn Care*. London, Edinburgh, New York, Philadelphia, St. Louis, Sidney, Toronto, 2002; p. 16-32.
- [2] Sarhadi NS, Murray GD, Reid WH. Trends in burn admissions in Scotland during 1970–1992. *Burns* 1995; 21: 612–5.
- [3] Carvajal HF. Fluid therapy for the acutely burned child. *Comp Ther* 1977; 3: 17–24.
- [4] Curreri PW, Richmond D, Marvin J, Baxter CR. Dietary requirements of patients with major burns. *J Am Diet Assoc* 1974; 65: 415–7.
- [5] Hildreth MA, Herndon DN, Desai MH, Duke MA. Reassessing caloric requirements in pediatric burn patients. *J Burn Care Rehabil* 1988; 9: 616–8.
- [6] Jackson MP, Philp B, Murdoch LJ, Powell BWEM. High frequency oscillatory ventilation

- successfully used to treat a severe paediatric inhalation injury. *Burns* 2002; 28: 509–11.
- [7] Herndon DN, Barrow RE, Rutan RL, Rutan TC, Desai MH, Abston S. A comparison of conservative versus early excision. Therapies in severely burned patients. *Ann Surg* 1989; 209: 547–53.
- [8] Wilmore DW, Long JM, Mason Jr AD, Skreen RW, Pruitt Jr BA. Catecholamines: mediator of the hypermetabolic response to thermal injury. *Ann Surg* 1974; 180: 653–69.
- [9] Sheridan R. Specific therapies for inhalation injury. *Crit. Care Med.* 2002; 30: 718–9.
- [10] Guy JS, Peck MD. Smoke inhalation injury: pulmonary implications. *Respir Care* 1999; 3: 904–12.
- [11] Demling RH. Smoke inhalation injury. In: Shoemaker W, editor. *Textbook of critical care*. PA, USA: WB Saunders Company, 1995; p. 1506.
- [12] Moritz AR, Henriques FC, McLean R. The effects of inhaled heat on the air passages and lungs-an experimental investigation. *M. J. Path.* 1945; 2: 311–31.
- [13] Moritz AR, Weisinger JR. The effects of cold air on the air passages and lungs. *Archives of Internal Medicine.* 1945; 75: 233–40.
- [14] Hanna LM, Scherer PW. A theoretical model of localized heat and water vapor transport in the human respiratory tract. *ASME Journal of Biomechanical Engineering.* 1986; 108: 19–27.
- [15] Hanna LM, Scherer PW. Measurement of local mass transfer coefficients in a cast model of the human upper respiratory tract. *ASME Journal of Biomechanical Engineering.* 1986; 108: 12–8.
- [16] Nuckolis ML, Zumrick JL, Johnson CE. Heat and water vapor transport in the human upper airways at hyperbaric conditions. *ASME Journal of Biomechanical Engineering.* 1983; 105: 24–30.
- [17] Saidel GM, Kruse KL, Primiano FP. Model simulation of heat and water vapor transport dynamics in an airway. *ASME Journal of Biomechanical Engineering.* 1983; 105: 188–93.
- [18] Liu J, Wang C. *Bioheat Transfer*. 1<sup>st</sup> ed. Beijing: Science Press, 1997 [in Chinese]
- [19] Zhao RY, Fan CY, Xie DH, Qian YM. *Air Conditioning*. Third ed. Beijing: Architecture and Building Press, 1998 [in Chinese]
- [20] Li A, Yang ZY. *Inhalation Injury*. 1<sup>st</sup> ed. Beijing: People's Military Medical Press, 1993 [in Chinese]
- [21] Torvi DA, Dale JD. A finite element model of skin subjected to a flash fire. *ASME J. Biomech Eng.* 1994; 116: 250–5.
- [22] Henriques FC, Moritz AR. Studies of thermal injury, I. The conduction of heat to and through skin and the temperatures attained therein. A theoretical and an experimental investigation. *Amer. J. Pathol.* 1947; 23: 531–49.

## Figures and legends

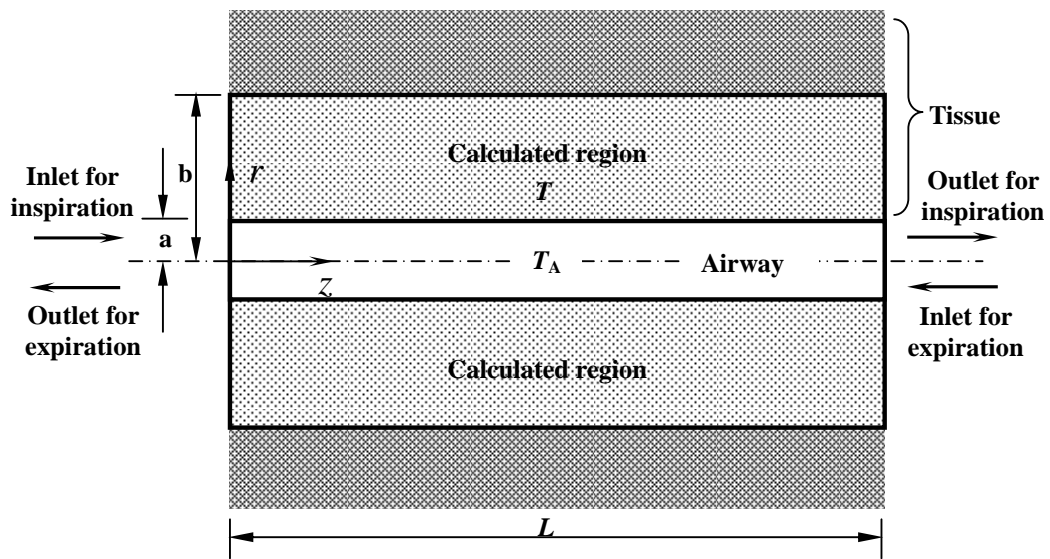


Fig. 1. Schematic model for the respiratory tract (idealized trachea).

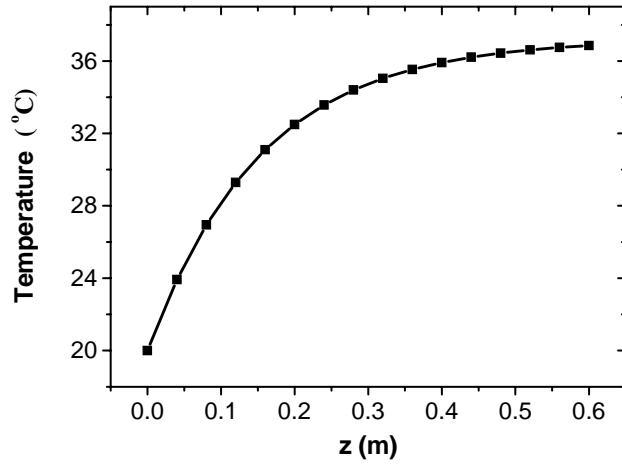


Fig. 2. Steady state temperature distribution of tissue along the airway in normal conditions.

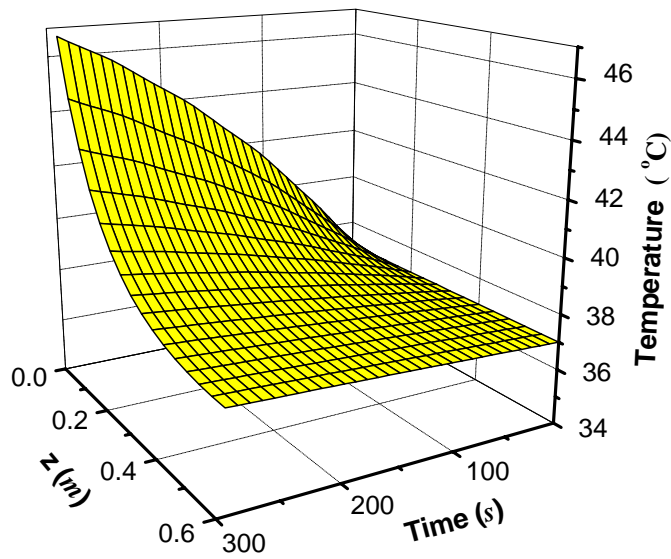


Fig. 3. Transient tissue temperature profile during a fire ( $K=0.5 \text{ W/m}\cdot\text{K}$ ,  $W_b=0.5 \text{ kg/m}^3\cdot\text{s}$ ,

$$Q_m=420 \text{ W/m}^3, T_f=100^\circ\text{C}, V=300\text{cm}^3/\text{s}, \varphi=0.3, T^*=3\text{s}).$$

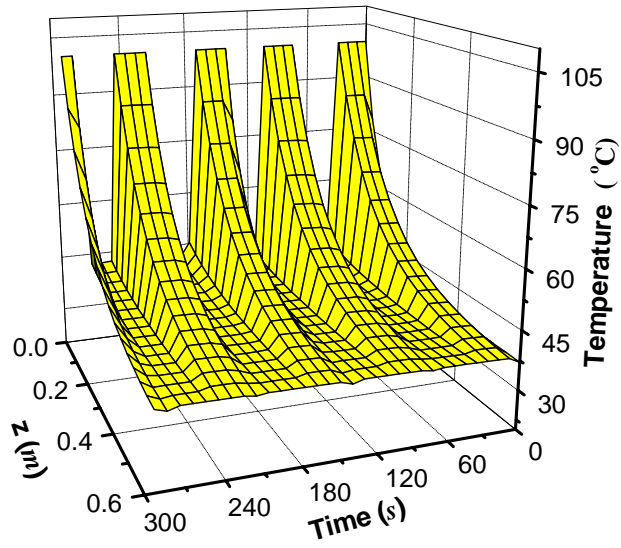
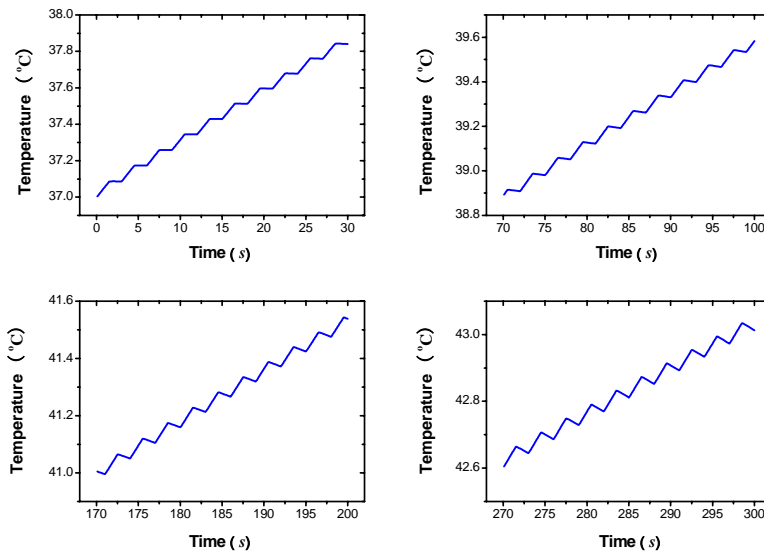
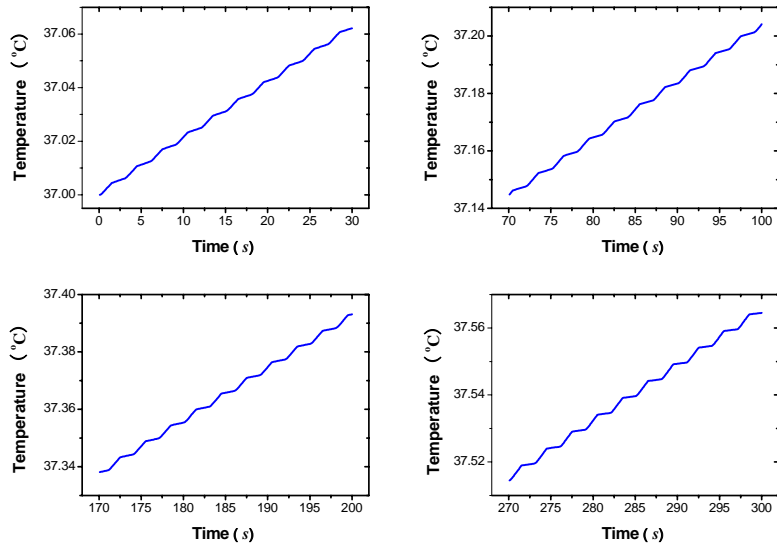


Fig. 4. Transient air temperature distribution during a fire ( $K=0.5 \text{ W/m} \cdot \text{K}$ ,  $W_b=0.5 \text{ kg/m}^3 \cdot \text{s}$ ,

$$Q_m=420 \text{ W/m}^3, T_f=100^\circ \text{C}, V=300 \text{ cm}^3/\text{s}, \varphi=0.3, T^*=3\text{s}).$$



(a)

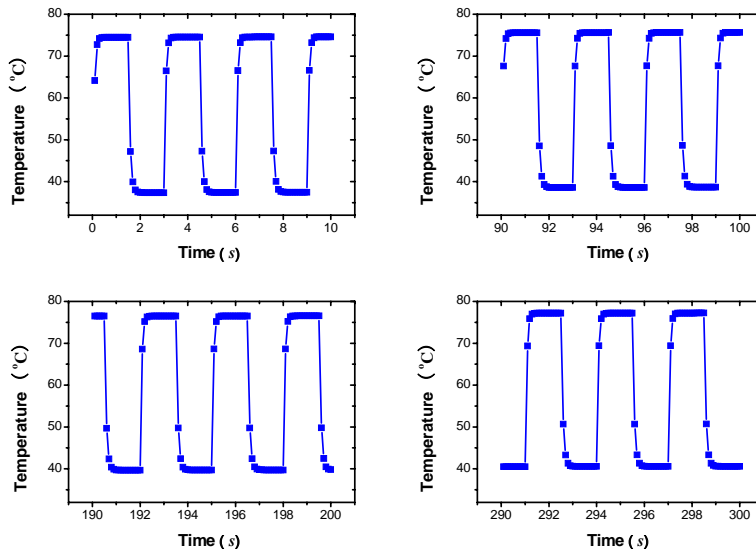


(b)

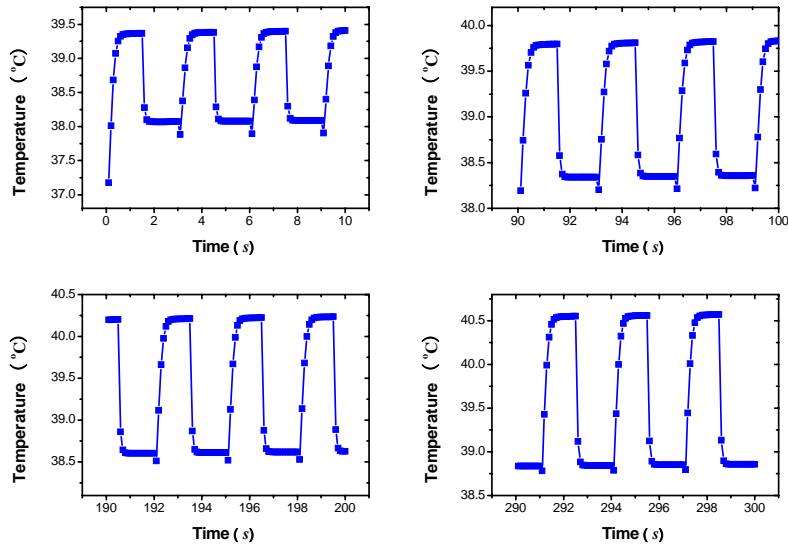
Fig. 5. Transient tissue temperature responses at two specific positions (a)  $z = 8\text{cm}$ ,  $r = 0.635\text{cm}$  and (b)  $z = 52\text{cm}$ ,  $r = 0.635\text{cm}$ .

( $K=0.5\text{ W/m}\cdot\text{K}$ ,  $W_b=0.5\text{ kg/m}^3\cdot\text{s}$ ,  $Q_m=420\text{ W/m}^3$ ,  $T_f=100^{\circ}\text{C}$ ,  $V=300\text{cm}^3/\text{s}$ ,  $\varphi=0.3$ ,

$T^*=3\text{s}$ )



(a)



(b)

Fig. 6. Transient air temperature responses at two sections  $z = 8\text{cm}$  (a) and  $z = 52\text{cm}$  (b).

$$(K = 0.5 \text{ W/m} \cdot \text{K}, W_b = 0.5 \text{ kg/m}^3 \cdot \text{s}, Q_m = 420 \text{ W/m}^3, T_f = 100^\circ \text{C}, \\ V = 300 \text{ cm}^3/\text{s}, \varphi = 0.3, T^* = 3\text{s})$$

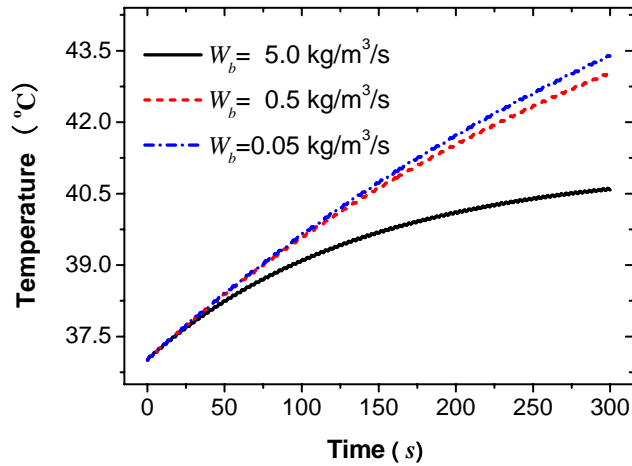


Fig. 7. Effect of blood perfusion levels on temperature response at a specific position ( $z = 8\text{cm}, r = 0.635\text{cm}$ ).

$$(K = 0.5 \text{ W/m} \cdot \text{K}, Q_m = 420 \text{ W/m}^3, T_f = 100^\circ \text{C}, V = 300 \text{ cm}^3/\text{s}, \varphi = 0.3, T^* = 3\text{s})$$

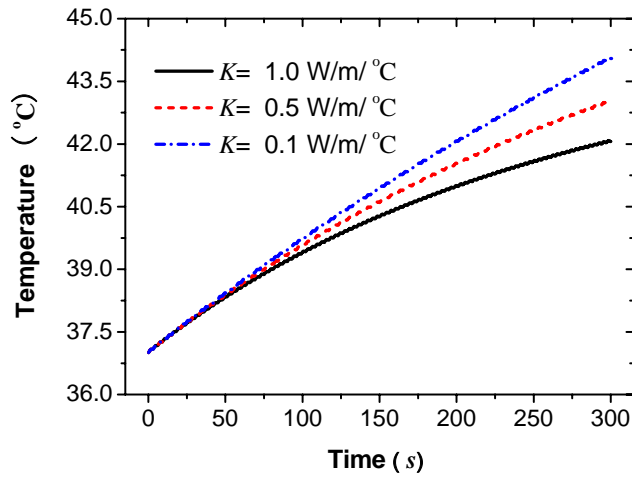


Fig. 8. Effect of thermal conductivity of tissues on temperature response at a specific position ( $z = 8\text{cm}$ ,  $r = 0.635\text{cm}$ ).

$$(W_b = 0.5 \text{ kg/m}^3 \cdot \text{s}, Q_m = 420 \text{ W/m}^3, T_f = 100^\circ\text{C}, V = 300\text{cm}^3/\text{s}, \varphi = 0.3, T^* = 3\text{s})$$

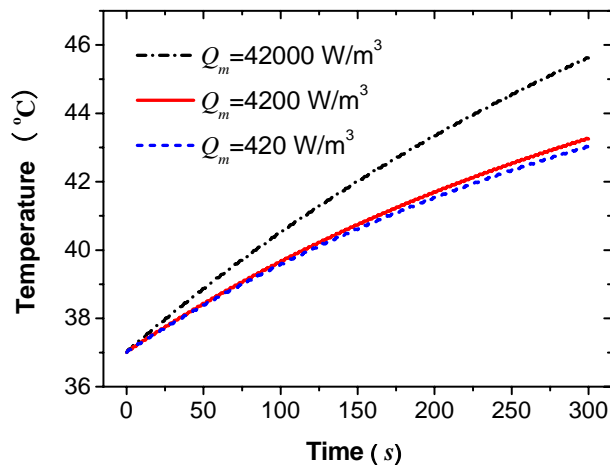


Fig. 9. Effect of metabolic rate of tissues on temperature response at a specific position ( $z = 8\text{cm}$ ,  $r = 0.635\text{cm}$ ).

$$(K = 0.5 \text{ W/m} \cdot \text{K}, W_b = 0.5 \text{ kg/m}^3 \cdot \text{s}, T_f = 100^\circ\text{C}, V = 300\text{cm}^3/\text{s}, \varphi = 0.3, T^* = 3\text{s})$$

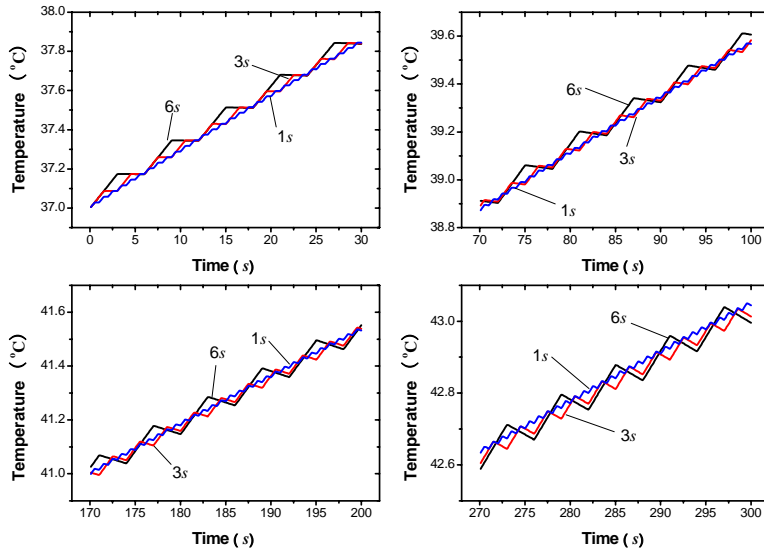


Fig. 10. Effect of respiratory frequency on temperature response at a specific position.

$(z = 8\text{cm}, r = 0.635\text{cm}) (K = 0.5 \text{ W/m}\cdot\text{K}, W_b = 0.5 \text{ kg/m}^3 \cdot \text{s}, Q_m = 420 \text{ W/m}^3,$

$$T_f = 100^\circ\text{C}, V = 300\text{cm}^3/\text{s}, \varphi = 0.3, T^* = 3\text{s})$$

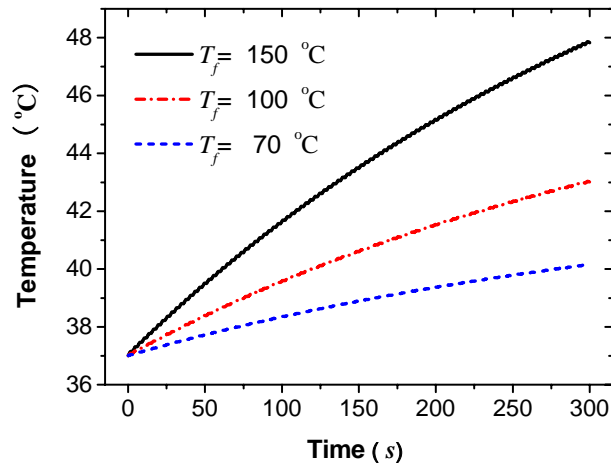


Fig. 11. Effect of surrounding air temperature on temperature response at a specific position

$(z = 8\text{cm}, r = 0.635\text{cm}).$

$(K = 0.5 \text{ W/m}\cdot\text{K}, W_b = 0.5 \text{ kg/m}^3 \cdot \text{s}, Q_m = 420 \text{ W/m}^3, V = 300\text{cm}^3/\text{s}, \varphi = 0.3, T^* = 3\text{s})$

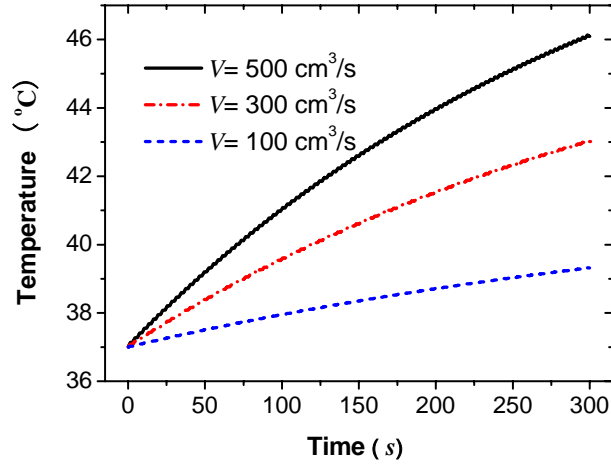


Fig. 12. Effect of local mean longitudinal air velocity on temperature response at a specific position ( $z = 8\text{cm}$ ,  $r = 0.635\text{cm}$ ).

( $K = 0.5 \text{ W/m}\cdot\text{K}$ ,  $W_b = 0.5 \text{ kg/m}^3\cdot\text{s}$ ,  $Q_m = 420 \text{ W/m}^3$ ,  $T_f = 100^\circ\text{C}$ ,  $\varphi = 0.3$ ,  $T^* = 3\text{s}$ )

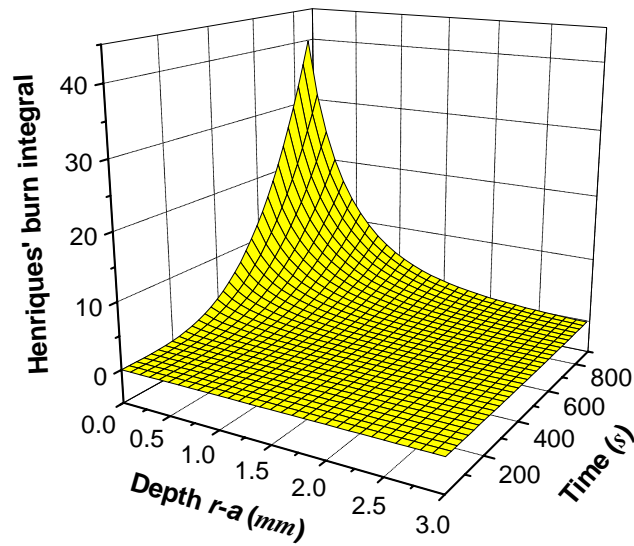


Fig. 13. Dimensionless Henriques' burn integral distribution at the surface of tissue. ( $0.635\text{cm} \leq r \leq 3.635\text{cm}$ ) during a fire ( $K = 0.5 \text{ W/m}\cdot\text{K}$ ,  $W_b = 0.5 \text{ kg/m}^3\cdot\text{s}$ ,  $Q_m = 420 \text{ W/m}^3$ ,  $T_f = 100^\circ\text{C}$ ,  $V = 300\text{cm}^3/\text{s}$ ,  $\varphi = 0.3$ ,  $T^* = 3\text{s}$ )

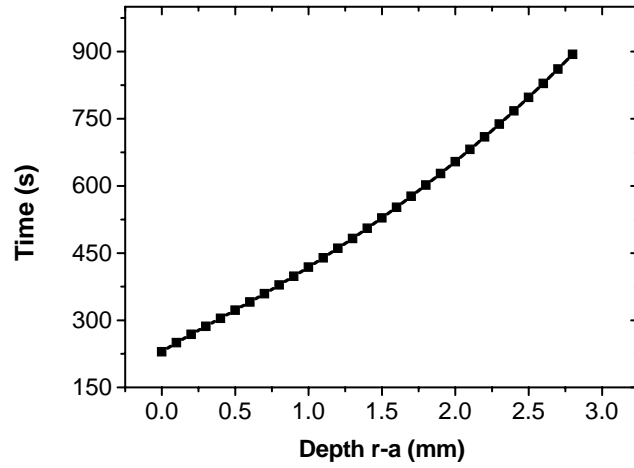


Fig. 14. Time prediction of the first-degree burn at the surface of tissue ( $0.635\text{cm} \leq r \leq 3.635\text{cm}$ ) during a fire ( $K=0.5 \text{ W/m} \cdot \text{K}$ ,  $W_b=0.5 \text{ kg/m}^3 \cdot \text{s}$ ,  $Q_m=420 \text{ W/m}^3$ ,  $T_f=100^\circ \text{C}$ ,  $V=300\text{cm}^3/\text{s}$ ,  $\varphi=0.3$ ,  $T^*=3\text{s}$ ).

Table 1 Constant for the first and second-degree burns integral [1]

Epidermis	Henriques' constant	Weaver's constant	Mehta's constant
$P$ ( $\text{s}^{-1}$ )	$3.1 \times 10^{98}$	$3.1 \times 10^{98}$ , $44^\circ \text{C} < T \leq 50^\circ \text{C}$ $1.823 \times 10^{51}$ , $T \geq 50^\circ \text{C}$	$1.43 \times 10^{72}$
$\Delta E / R$ (K)	75000	93534.9, $44^\circ \text{C} < T \leq 50^\circ \text{C}$ 39109.8, $T \geq 50^\circ \text{C}$	55000